Influence of oxygen-ordering kinetics on Raman and optical response in $YBa_2Cu_3O_{6.4}$

A. A. Maksimov, D. A. Pronin, S. V. Zaitsev, and I. I. Tartakovskii
Institute of Solid State Physics, Russian Academy of Sciences, Chernogolovka, Moscow district, 142432, Russia

G. Blumberg
NSF Science and Technology Center for Superconductivity and Department of Physics, University of Illinois at Urbana-Champaign, Urbana, Illinois, 61801-3080
and Institute of Chemical Physics and Biophysics, Rävala 10, Tallinn EE0001, Estonia

M. V. Klein, M. Karlow, and S. L. Cooper
NSF Science and Technology Center for Superconductivity and Department of Physics, University of Illinois at Urbana-Champaign, Urbana, Illinois, 61801-3080

A. P. Paulikas and B. W. Veal
Materials Science Division, Argonne National Laboratory, Argonne, Illinois, 60439
(Received 24 June 1996)

Kinetics of the optical and Raman response in $YBa_2Cu_3O_{6.4}$ were studied during room-temperature annealing following heat treatment. The superconducting T_c, dc resistivity, and low-energy optical conductivity recover slowly, implying a long relaxation time for the carrier density. Short relaxation times are observed for the B_{1g} Raman scattering—magnetic, continuum, and phonon—and the charge transfer band. Monte Carlo simulations suggest that these two relaxation rates are related to two length scales corresponding to local oxygen ordering (fast) and long chain and twin formation (slow). [S0163-1829(96)50734-4]

Hole doping in $YBa_2Cu_3O_{6+x}$ for $x>0$ occurs through occupancy of oxygen chain sites in the CuO-chain layer. As a result, holes transfer to the $Cu(2)O_2$-plane layer, where most of the metallic and superconducting properties have their origin. Chain-site oxygen vacancies ($x<1$) locally affect the planes; for instance, they cause a charge redistribution around the plane-site Cu(2)'s, the effect of which is to broaden the Cu(2) nuclear quadrupole resonance (NQR) line.[1] The present work uses time-dependent annealing to study how several other plane-related properties respond to changes in chain-site oxygen disorder. Room temperature (RT) annealing has been observed in oxygen deficient $YBa_2Cu_3O_{6+x}$ single crystals rapidly quenched from elevated temperatures ($T\approx 420$ K) (Ref. 2). It is generally believed that the disorder produced by heating is frozen by the fast quench, and that RT annealing results from reordering of oxygen in the CuO-chain layer via diffusion. The reordering lowers the average valence of the chain Cu and transfers holes to the CuO_2 plains.[3] Thus far, the influence of RT annealing has been seen experimentally in the superconducting transition temperature, T_c (Ref. 2), the Raman two-magnon line (2-ML) and electronic continuum intensity,[4] and various structural[5] and optical[6] parameters. However, a detailed understanding of the kinetics involved has yet to be achieved.

We have investigated the kinetics of several physical properties of underdoped $YBa_2Cu_3O_{6.4}$ on the same sample during reproducible quench/anneal cycles, and find two characteristic behaviors. One is exhibited by the dc resistivity, T_c, and the low-frequency (LF) optical spectral weight, all of which recover slowly over a few days following heat treatment. In sharp contrast, the optical charge-transfer band (CTB), the B_{1g} Raman 2-ML, electronic continuum, and phonon intensity relax rapidly during the first hours of RT annealing. Since the dc resistivity and T_c involve the CuO_2-plane carrier density directly, our results suggest that the rapid relaxation of the second group occurs through a process that is independent of chain-to-plane charge transfer.

Monte Carlo simulations of oxygen ordering in the chains also show two relaxation rates: one fast, corresponding to short-range oxygen order where the correlation length is of order the lattice constant, $r\approx a$; and one slow, where the correlation length is large compared to a. We infer that the fast relaxation processes depend on short-range correlations, whereas long-range oxygen order is important to the slower processes.

The inset of Fig. 1 shows that our $YBa_2Cu_3O_{6.4}$ single crystal displays a sharp superconducting transition ($\Delta T_c \lesssim 1-1.5$ K) at each quench/anneal cycle, despite T_c changes from 18 K before the thermal treatment to 2.9 K immediately following the quench. The reproducibility of these results for many cycles indicates that the total oxygen content of the sample remains constant. The homogeneity of the oxygen distribution at the 1 μm level was confirmed by micro-Raman experiments.

The optical reflectance at near-normal incidence in the energy range $\omega = 0.03$–2.25 eV was measured at successive times following thermal treatment using a rapid-scan Michelson interferometer. A Kramers-Kronig transformation[7] was applied to obtain the optical conductivity $\sigma(t,\omega)$ from the measured reflectance data. Since variations in the high frequency reflectance ($3.8<\omega<4.3$ eV) (Ref. 6) cause changes of less then 5% in the conductivity $\sigma(t,\omega)$ for $\omega<2.5$ eV, ellipsometric data measured after complete relaxation were

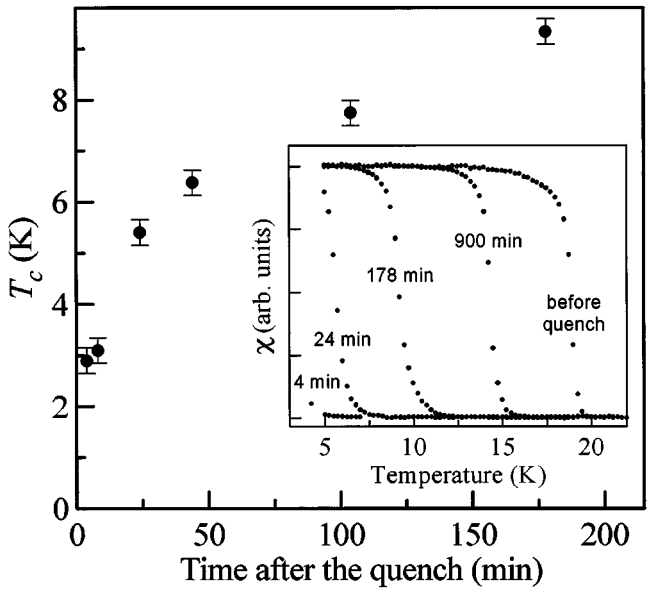

FIG. 1. Temporal dependencies of T_c after the quench. Inset: Dependence of magnetic susceptibility χ on temperature measured at different times after the quench.

used in the energy range $\omega = 2.25-6$ eV to make this transformation. The inset of Fig. 2 shows $\sigma(t,\omega)$ for $YBa_2Cu_3O_{6.4}$ at two times t following the quench, $t_0 = 10$ min and t_∞ (fully relaxed). Immediately after the quench, the

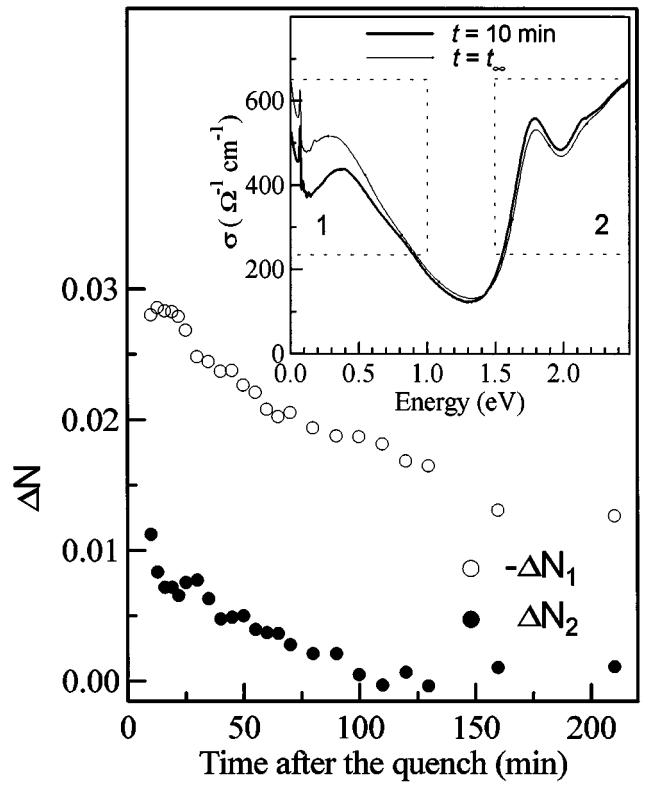

FIG. 2. Temporal dependencies after the quench of the variation in the optical conductivity integrated over the LF (open circles) and CTB (filled circles) regions. Inset: Optical conductivity $\sigma(t,\omega)$ before the heat treatment and 10 min after the quench. Boxes 1 and 2 show the integration regions.

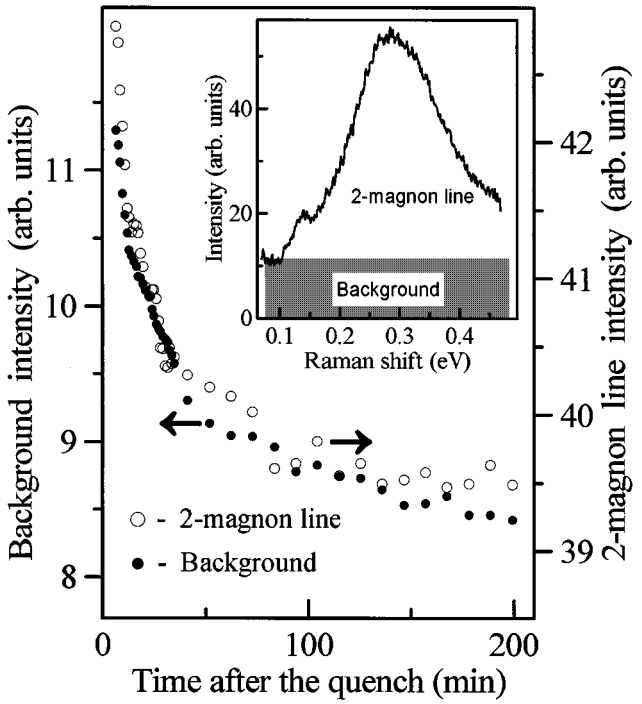

FIG. 3. Temporal dependencies of the intensity of the two-magnon Raman scattering line maximum (open circles) and the background intensity (filled circles) after the quench. The vertical axis scales are anchored to the time axis at their prequench values (i.e., 7.7 for background and 38.5 for 2-ML). Inset: Raman spectrum measured in $x'y'$ geometry at $t = 6$ min after the quench. Filled region corresponds to broad structureless electronic background.

largest changes in $\sigma(t,\omega)$ are a decrease in the LF spectral weight (box 1 in the inset), and an increase in the CTB spectral weight (box 2) (Ref. 9). The LF spectral weight (box 1) is comprised of a Drude part due to holes in the CuO_2 planes plus a mid-IR peak associated with chain conductivity.[8] In Fig. 2 we plot as a function of time the variation in effective number of carriers (integrated spectral weight), $\Delta N_{1,2}(t) = C\int_{\text{box1,2}}[\sigma(t,\omega)-\sigma(t_\infty,\omega)]d\omega$, where the constant C is given in Eq. (3) of Ref. 9. We find that $\Delta N_2(t)$ takes $\approx$100 min to recover to its initial value, whereas complete recovery of $\Delta N_1(t)$ requires several days. Moreover, the sum $\Delta N(t) = \Delta N_1(t) + \Delta N_2(t)$ during the first $\sim$100 min remains approximately constant. These results signify that the transfer of spectral weight from the CTB to LF band occurs quite rapidly relative to the time scale associated with chain-to-plane charge transfer which causes an increase in $\Delta N_1(t)$ due to increased in-plane carrier density (real doping). Notably, the monotonic increase in $\Delta N_1(t)$ at long times may reflect different effective masses for holes in the chain and the plane layers.

Raman-scattering (RS) data from single-crystal $YBa_2Cu_3O_{6.4}$ were obtained in 20 s intervals at successive times following the quench using a CCD equipped Raman triple spectrometer. The 2-ML (Refs. 10 and 11) and electronic continuum [11,12] spectra were obtained at room temperature, while the 336 cm^{-1} phonon-scattering data were taken at 5 K. The inset of Fig. 3 presents the RS spectrum measured at $t_0 = 6$ min after the quench in the $x'y'$ (mainly

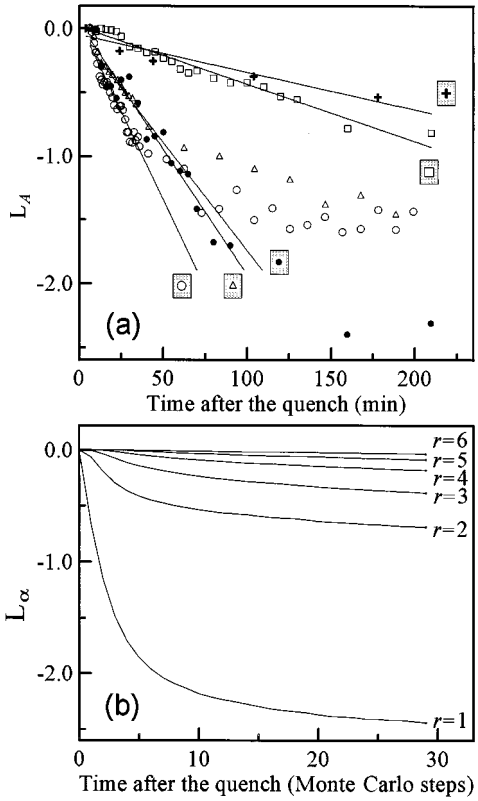

FIG. 4. (a) Measured values $L_A(t)$ [Eq. (1)] for parameters in Figs. 1–3. Straight lines are the results of least-squares fitting of experimental data at the initial stage of aging. Crosses: T_c, $\tau\approx340$ min; squares: $\Delta N_1(t)$, $\tau\approx220$ min; filled circles: $\Delta N_2(t)$, $\tau\approx59$ min; triangles: background, $\tau\approx51$ min; open circles: two-magnon line, $\tau\approx36$ min. (b) Time dependencies of L_α for calculated parameter α in $YBa_2Cu_3O_{6.4}$ crystals for different correlation distances $1\leqslant r\leqslant 6$ in units of $\sqrt{2}a$.

B_{1g}) geometry. Fig. 3 shows the temporal dependence of the 2-ML and electronic background (0.1 to 0.5 eV) intensities. An increase of both the 2-ML and low-frequency RS background intensities is observed after quenching; however, the fractional increase is larger for the background than for the 2-ML. Interestingly, the main change in the intensity for both features occurs during the initial 50–100 min, although complete recovery to prequench values takes several days.

At least two characteristic relaxation rates may be extracted from Figs. 1–3 if an exponential temporal dependence of the form $A(t)-A(t_\infty)=[A(t_0)-A(t_\infty)]\exp(-t/\tau)$ is assumed. In order to estimate these times, we have represented the data as

$$L_A(t)\equiv\ln\left|\frac{A(t)-A(t_\infty)}{A(t_0)-A(t_\infty)}\right|, \tag{1}$$

where $A(t)$ is one of the measurable quantities and $A(t_0)$ is the first measured value of A just after the quenching.

Figure 4(a) plots $L_A(t)$ for the optical and RS quantities, and T_c. Two distinct relaxation behaviors are clearly seen. The kinetics of T_c and $\Delta N_1(t)$ demonstrate a single long relaxation time, estimated to be $\tau\approx250$ min via a straight line least squares fit to the experimental points in the range $t=0-200$ min. In Ref. 13, the kinetics of the dc resistivity and T_c during room-temperature annealing were shown to be of the same order. By contrast, the kinetics of 2-ML, background intensity, the integrated intensity of the B_{1g} phonon and $\sigma_t(\omega)$ in the CTB spectral region demonstrate two relaxation times: an initially short relaxation ($\tau\approx50$ min) over the first ≈100 min, followed by a considerably slower relaxation.

We attribute the observed kinetics of the several physical properties to diffusion-induced reordering of oxygen in the chain layers. The fast and slow kinetics seen in the initial stages of relaxation are assigned to oxygen ordering with correspondingly short and long correlation lengths. To gain further insight, we carried out a Monte Carlo simulation of the oxygen distribution kinetics in the CuO chains of $YBa_2Cu_3O_{6+x}$. We used the asymmetric next-nearest-neighbor Ising model,[14] which takes into account three different effective pair interactions between oxygen atoms ($V_1=367$ meV, $V_2=-0.348V_1$, and $V_3=0.159V_1$) (Ref. 15). This model has been used previously[15,16] to show kinetics of chain-oxygen order and also to determine final oxygen structure.[17,18] We parametrize the results of these simulations in terms of a parameter α, which measures how close the structure is to the ordered Ortho-I (OI) phase.[19] α is defined to be zero when the structure is fully disordered and unity when the structure is in the ideal OI phase. We calculate α for different correlation distances r by comparing, at every oxygen position, the Monte Carlo oxygen arrangement on a square of side $2r$ to the perfect OI structure. We used up to 5000 Monte Carlo steps on a 128×128 lattice at room temperature, starting with a disordered structure. To compare the calculated and experimental data we defined function $L_\alpha(t)$ for the ordering parameter α similar to $L_A(t)$ [Eq. (1)], where t_∞ equals to 5000 Monte Carlo steps. Fig. 4(b) shows the time dependence of L_α for different correlation distances r with oxygen content $x=0.4$. It is seen that the dependence of L_α on time for different r mimics the temporal dependence of the various measured quantities. For long correlation distances, L_α demonstrates slow kinetics, whereas the time dependencies of L_α for short distances ($r=1$–2) demonstrate two rates: fast for the initial stage and much slower at longer times. These two relaxation rates result from the fact that at the initial stage of relaxation only local ordering takes place. Consequently, many little twins (a few lattice constants in size) appear. This fast process is associated with short correlation lengths r, and the slower kinetics correspond to motion of twin walls which results in the subduction of smaller twins by larger ones. This process is revealed at all correlation distances.[19] Similar results hold for the Ortho-II ordering parameter. As expected, calculations performed for higher values of the oxygen content show less difference between the kinetics at various correlation distances.

The long relaxation times exhibited by the dc conductivity,[13] T_c and $\Delta N_1(t)$ imply that the fast kinetic behavior displayed by the CTB and the B_{1g} RS features occurs before oxygen ordering in the chains causes significant hole transfer to the CuO_2 planes. Since some rapidly annealing parameters, such as the 2-ML, are believed to have their

origins in the planes, *we conclude that short-range oxygen ordering in the chains gives rise to short-length-scale changes in the planes without significantly altering the average planar carrier density.*

Comparing Fig. 4(a) with Fig. 4(b), one can conclude that the kinetics for $\Delta N_2(t)$ and for the B_{1g} symmetry RS are determined by local oxygen ordering at nearest-neighbor distances. As discussed in Ref. 9 the CTB is most probably due to a local excitation of a hole in the CuO_2 planes from Cu(2) $d_{x^2-y^2}$ to the four O(2,3) $p_{x,y}$ states that surround a first-neighbor Cu(2) site. The rapid transfer of the integrated spectral weight from $\Delta N_2(t)$ to $\Delta N_1(t)$ suggests partial delocalization of bound carriers.

The 2-ML mainly probes short wavelength magnetic excitations from the vicinity of the magnetic Brillouin zone boundary $\mathbf{k}=(\pi/a,0)$, which occur via photon-driven superexchange between two nearest-neighboring Cu(2) spins in the antiferromagnetic surroundings. Thus, the CTB and 2-ML both require only short-range antiferromagnetic order which is affected by changes in the local carrier distribution but is independent of the average carrier number. The rather fast kinetics of the Raman B_{1g} continuum implies that it is also a local excitation, perhaps of magnetic origin, *and that it is not related directly to the average carrier number.* Phonon interaction with the continuum might explain the observed phonon line intensity kinetics through a Fano-type effect, but a detailed model needs to be formulated to understand this. By contrast, the resistivity, T_c, and the LF absorption kinetics are determined by longer distance oxygen ordering connected with the formation of ordered oxygen chains several lattice constants long. The LF band has been shown to be polarized along the chain direction;[9] thus chain fragments of a minimum length are required for this band to occur. Since T_c requires coherence over a distance equal to the superconducting correlation length ξ_0, the similarity of annealing kinetics leads us to conclude that the LF absorption band and the resistivity changes have their origins in phenomena occurring on length scales that are similar to ξ_0 and that are several times larger than those responsible for the Raman features and the CTB.

In summary, we have measured the kinetic behavior of the magnetic susceptibility, the B_{1g} symmetry Raman scattering (2-ML, electronic continuum and the 336 cm^{-1} phonon), and the optical conductivity (LF and CTB) of $YBa_2Cu_3O_{6.4}$ single crystals during room-temperature annealing. The kinetics of the Raman features and the optical conductivity in the CTB region demonstrate fast relaxation ($\tau_f \sim 50$ min). The relaxation time for the resistivity, the LF absorption, and T_c is much larger ($\tau_s \gtrsim 220$ min), implying that there is a nearly constant average carrier number for times less than τ_f. Comparing the measured kinetics with Monte Carlo model simulations we suggest that the short-length-scale excitations are responsible for the fast processes, such as B_{1g} symmetry RS and the CTB in the optical conductivity. Longer correlations ($r>2$) are responsible for changing the resistivity, LF optical conductivity and hence the effective carrier concentration. We conclude that several properties of the electronic system in the CuO_2 planes are strongly influenced by the disorder in CuO chains, confirming and extending the earlier NQR work.[1] It would be interesting to study the annealing kinetics of NQR linewidths and data from other local probes. The CuO_2 planes in $YBa_2Cu_3O_{6+x}$ for $x<1$ should not be considered to be ''ideal''; significant fluctuations in potential play an important role in various physical properties. The kinetics shown by these properties upon RT annealing provides a new approach for their study in $YBa_2Cu_3O_{6+x}$ and perhaps in other high-T_c superconductors and related materials.

The joint Russian/U.S. work was supported by NATO CRG Grant No. 92-1239, the work at Chernogolovka by RBRF 95-02-06111a, ISF NKW000, and RSP on HTSC 93193, the work at Urbana by NSF DMR Grant No. 91-20000 through STCS, and the work at Argonne by U.S. DOE Grant No. W-31-109-ENG-38.

[1] H. Schiefer *et al.*, Physica C **162-164**, 171 (1989).
[2] B. W. Veal *et al.*, Phys. Rev. B **42**, 6305 (1990).
[3] G. Uimin and J. Rossat-Mignod, Physica C **199**, 251 (1992).
[4] A. A. Maksimov *et al.*, Phys. Rev. B **49**, 15 385 (1994).
[5] J. D. Jorgensen *et al.*, Physica C **167**, 571 (1990).
[6] J. Kircher *et al.* Phys. Rev. B **46**, 588 (1992).
[7] F. Stern, *Solid State Physics* (Academic, New York, 1963), Vol. 15.
[8] K. Widder *et al.*, Physica C **232**, 82 (1994).
[9] S. L. Cooper *et al.*, Phys. Rev. B **47**, 8233 (1993).
[10] K. B. Lyons *et al.*, Phys. Rev. B **37**, 2353 (1987); K. B. Lyons *et al.*, Phys. Rev. Lett. **60**, 732 (1988).
[11] G. Blumberg *et al.*, Phys. Rev. B **49**, 13 295 (1994).
[12] D. Reznik *et al.*, Phys. Rev. B **48**, 7624 (1993).
[13] B .W. Veal and Chun Gu, J. Electron Spectrosc. Relat. Phenom. **66**, 321 (1994).
[14] E. Salomons and D. de Fontaine, Phys. Rev. B **41**, 11 159 (1990).
[15] H. F. Poulsen *et al.*, Phys. Rev. Lett. **66**, 465 (1991).
[16] G. Ceder, R. McCormack, and D. de Fontaine, Phys. Rev. B **44**, 2377 (1991).
[17] R. McCormack, D. de Fontaine, and G. Ceder, Phys. Rev. B **45**, 12 976 (1992).
[18] H. F. Poulsen *et al.*, Nature Lett. **349**, 594 (1991).
[19] A. A. Maksimov, D. A. Pronin, S. V. Zaitsev, and I. I. Tartakovskii (unpublished).